Compressive Sensing-Based Optimal Reactive Power Control of a Multi-Area Power System

IRFAN KHAN[1,2], (Student Member, IEEE), YINLIANG XU[3,4], (Member, IEEE), SOUMMYA KAR[1], (Member, IEEE), AND HONGBIN SUN[3,4], (Senior Member, IEEE)

[1]Electrical and Computer Engineering Department, Carnegie Mellon University, Pittsburgh, PA 15213, USA
[2]School of Electronics and Information Technology, Sun Yat-sen University, Guangzhou 510275, China
[3]Tsinghua-Berkeley Shenzhen Institute, Shenzhen 518055, China
[4]Department of Electrical Engineering, State Key Laboratory of Power Systems, Tsinghua University, Beijing 100084, China

Corresponding author: Yinliang Xu (xu.yinliang@sz.tsinghua.edu.cn)

ABSTRACT To deal with the increasing load demand and environmental effects of conventional power devices, power system has become an enlarged complex network with the integration of distributed generators. Real-time control of power system now needs a massive amount of information to be transmitted between each local device and the central controller. The transmission of a huge quantity of information data poses great challenge to the communication network. To deal with this issue in reactive power control, this paper proposes a novel real-time compressive sensing-based optimal reactive power control of a multi-area interconnected power system. The objective is to minimize the power loss, voltage deviation, and reactive power generation cost simultaneously. According to the proposed scheme, the measured data in each control area is compressed before being transmitted through the communication network, and then recovered accurately by the discrete central controller. Orthogonal matching pursuit algorithm is adopted to recover the compressed data, owing to its fast convergence speed. Simulation results demonstrate the effectiveness of the proposed compressive sensing-based approach by significantly reducing the data size of the transmitted data.

INDEX TERMS Optimal reactive power control, compressive sensing, orthogonal matching pursuit algorithm, power loss, voltage deviation.

I. INTRODUCTION

For the reliable and stable operation of the power system, information of real-time parameters, state, and control variables of the whole power system shall be collected and processed. With the recent large-scale integration of Distributed Generation (DG) and introduction of smart meters in the power system, the volume of data that needs to be processed, has grown drastically [1]. According to [2], in 2014, 94 million smart meters were shipped worldwide and it is predicted that by 2022, the number of smart meters will reach 1.1 billion. When more and more devices are being connected to the same network segments, bandwidth becomes more limited with more network participants [2]. The synchrophasor data is reported on an N frames/s basis, where N can be selected between 1 and 120. Choosing a higher frame rate would further accelerate a demand for more bandwidth [3]. Power utilities often find it difficult to arrange large investments to build/upgrade communication networks to meet the

increased bandwidth demand [4]. Therefore, in this context, one must focus to achieve an efficient use of the existing communication channel bandwidth.

It is exhibited in [5] that the energy consumption by the communication channel increases significantly as the size of message to be transmitted increases in various applications of power grid. Furthermore, if the data package exceeds the maximum allowable data size, it needs to be divided into several smaller data packets, which may lead to considerable time delay. Therefore, it is advisable to decrease the size of real-time data for obvious reasons.

Reactive power control plays a vital role on power loss reduction and voltage control of the power system [6]. Under high penetration of new DG units, more and more reactive power control devices are being integrated into power grids. The large-scale deployment of these devices requires upgrading the existing reactive power control solutions [7]. Many conventional centralized algorithms have been employed to

solve the optimal reactive power control (ORPC) problem off-line [8], [9]. However, only few attempts have been made to control reactive power in real-time applications, which needs to upgrade the existing communication networks to meet with the increasing bandwidth demand.

To address the issue of fast two-way communication, decentralized ORPC techniques, which rely on local controllers only without explicit communication, have been proposed in [10] and [11]. An approximate measure for power loss is considered by controlling the reactive power generation from each DG in [10]. The authors in [11] demonstrated that total voltage deviation is higher using decentralized ORPC than that of using centralized ORPC. It is because of the reason that using decentralized control, each local DG controller tries to satisfy its local load demand while load buses without having their own reactive power generation sources, may happen to have large voltage deviation. Thus, due to the lack of broader available information, decentralized control may not be effective to coordinate all available resources in the network [12].

Recently, distributed ORPC techniques [7], [13], [14], which take advantage of sparse communication network, have been very popular among researchers. In [13], voltage regulation and power loss were minimized by adjusting the reactive power generation using a feedback strategy based distributed control algorithm. Minimization of the approximate power loss was proposed by controlling the bus voltages in [14], whereas in [7], authors proposed distributed multiple agent system based ORPC to optimize power loss and voltage deviation. It is shown that the data loss and communication delays may slow down the overall converging speed. Moreover, distributed algorithms require synchronized communication between the neighboring entities i.e. failing of the communication or delaying of information from even a single bus may slow down the distributed algorithm.

When comparing distributed and centralized schemes, it is found that centralized protocols show better performance in data loss recovery than the distributed protocols [15]. Also, the optimal solution of the centralized optimal control is found to be better than that of distributed optimal control [16], [17]. The reason may be that in distributed control, local information is shared among neighboring entities only, whereas in the centralized control, all the information of the system is known which ensures the better optimal control of reactive power. Also, most of the existing reactive power control solutions are centralized [7] and it is economical to improve the existing communication techniques than to completely reshape the overall communication paradigm. It may be expensive to deploy a controller on each DG bus.

Reactive power control service is mainly contemplated as a local control service because the reactive power may not be transmitted efficiently through long distances in transmission networks. Thus, it is usually suggested to control the voltage by using control devices dispersed throughout the power system. Therefore, system operators normally provide voltage control services from resources within their own controlled area [18], [19].

Although voltage control is primarily a local control problem, the recent two decades widespread blackouts have demonstrated that the voltage instability and collapse could be considered as an important factor in major power outages worldwide. It may involve several areas of an interconnected system and increase the scale of blackouts and even affect the intact areas [20], [21].

The multi-area power system without inter-area voltage coordination may be operated in a non-optimum state which means less security and stability margin. For instance, [22] reveals that in multi-area power systems, the optimization solution of an area for reducing the active power losses in its own region might lead to increase the losses globally in the interconnected system. Additional literature about the coordinated reactive power control in multi-area power system can be found in [23]–[29].

For centralized schemes, ORPC problem for a large power system requires a huge amount of data to be transmitted to the central controller. If the bandwidth of the communication network is not sufficiently large to support transmission of such massive amount of data, it may deteriorate the performance of the controller. To address the problem of limited bandwidth, recently, compressive sensing (CS) which takes advantage of sparse signal structures is considered as a promising joint data compression and reconstruction method to transmit information efficiently [30]. As the data obtained from observing a physical system like power system, inherently contains spatial and temporal correlation [31], it can be compressed before transmitting through the unreliable communication channel and recovered at the receiving end. A CS-based data loss recovery algorithm to improve the communication efficiency by reducing the communication burden and thus, saving the power demand is presented in [32], which is further improved in [33] with low space complexity, low floating-point calculations, and low time complexity robust CS framework. Recently, a data reduction scheme by removing redundant phasor information before transmission is proposed in [3] in order to reduce the amount of data.

To the authors' best knowledge, few attempts have been made to deploy advanced information processing techniques in the ORPC problem. In this paper, a centralized real-time ORPC is proposed for multi-area interconnected power system. Real-time data of bus voltages and line currents in each area is first sampled and compressed before being transmitted through the communication network. At the receiving end, it is first decoded and recovered accurately by the central controller. The size of the transmitted data can be significantly reduced with the use of CS. The proposed approach is reliable, robust and its effectiveness is validated through simulations. Major contributions of this paper are as follows:

1) Real-time optimal reactive power control of multi-area power system is solved to minimize power loss, voltage deviation and reactive power cost, simultaneously.

2) To meet with the challenges of high bandwidth requirement for real-time transmission of massive data of power system, compressive sensing technique is utilized to first compress the data package before transmitting it through the communication network and then recover it at the end of communication channel.

3) To deal with large control areas with huge amount of data, an Orthogonal Matching Pursuit algorithm is used to improve the reconstruction speed of the transmitted data.

4) Scalability of the proposed approach is investigated.

The rest of the paper is organized as follows. Section II formulates the CS based ORPC problem. Section III explains the working of compressive sensing. Section IV presents the proposed algorithm. Section V discusses the simulation results of the proposed control approach, and Section VI concludes the paper.

II. PROBLEM FORMULATION

Optimal reactive power control of DG plays a key role in the power system control and operation, which can lead to improved voltage profile, minimal active power loss and controllable reactive power generation cost. Therefore, the objective function to be optimize is formulized as:

$$\min_{Q_{Gi}} f_1(Q_{Gi}, V_i, \delta_i) = W_1 P_{loss} + W_2 D_V + W_3 C_Q \quad (1)$$

where W_1, W_2 and W_3 are the weight coefficients. P_{loss}, D_V and C_Q are the power loss, voltage deviation and cost of reactive power generation, respectively. Q_{Gi} is the total reactive power generation from each bus i. V_i and δ_i are the bus voltage magnitude and its angle on bus i respectively.

Expressions for the three sub-functions are given as:

$$P_{loss} = \sum_{i=1}^{n} \sum_{j=1}^{n} V_i V_j Y_{ij} \cos(\theta_{ij} + \delta_j - \delta_i) [34] \quad (2a)$$

$$D_V = \sum_{i=1}^{n} (V_i - V_i^*)^2 \quad (2b)$$

$$C_Q = \sum_{i=1}^{n} a_i Q_{G_i}^2 + b_i Q_{G_i} + c_i [35] \quad (2c)$$

where $Y_{ij} \angle \theta_{ij}$ is the element of admittance matrix. V_i^* is the reference voltage on bus i, whereas a_i, b_i and c_i are the reactive power cost coefficients. To minimize (1), admittance matrix, reference voltage and reactive power generation cost coefficients are usually fixed whereas, voltage phasors, and real & reactive power flows are the state measurements of the control area of power system as given in (3).

$$\mathbf{x}_i = \begin{bmatrix} V_i \angle \delta_i & P_{G_i} & Q_{G_i} \end{bmatrix}. \quad (3)$$

For minimization of (1) by a centralized approach, the state information is required to be transmitted to the central controller through communication channel. However, for real time ORPC, the communication channel bandwidth is usually limited and cannot execute the data transfer beyond
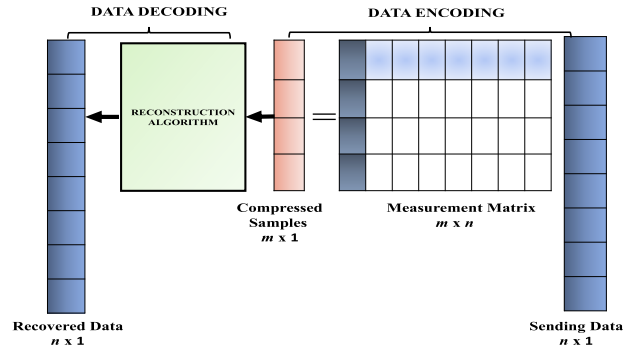

FIGURE 1. Encoding and decoding of measurement signal using CS.

its limit. To deal with this issue, in this paper, a compressive sensing based ORPC algorithm is proposed where state measurements data is first compressed before sending on to the communication channel and is recovered at the end of communication channel by the central controller. The theory of encoding and decoding of measurement signals using CS is explained in Fig. 1. At each time step k, the state measurements $\mathbf{x}(k)$ are taken from n sensors of the power system control area and compressed as (4)

$$\mathbf{y}(k) = \mathbf{\Phi}(k)\mathbf{x}(k) \quad (4)$$

where $\mathbf{x}(k)$ is the state information data of the control area, $\mathbf{y}(k)$ is the data after compression and $\mathbf{\Phi}(k) \in R^{m*n}$, is the measurement matrix at time step k where m is the number of samples after encoding while n is the number of samples before encoding. The value of n/m defines the compression ratio (ρ) of the CS.

At the end of communication channel the original n samples of $\mathbf{x}(k)$ can be recovered from m samples of $\mathbf{y}(k)$ measurements by solving ℓ_1-norm minimization problem as given in (5) [36]

$$\hat{\mathbf{x}}(k) = \arg\min_{\mathbf{x}(k)} \quad \|\mathbf{x}(k)\|_1$$
$$s.t. \quad \mathbf{y}(k) = \mathbf{\Phi}(k)\mathbf{x}(k). \quad (5)$$

where $\hat{\mathbf{x}}(k)$ is the recovered state information data. A number of methods can be used to solve the optimization problem in equation (5) [37], [38]. For real-time data recovery, matching pursuit methods [38] are preferred to prioritize the computational speed. Matching pursuit approximates the solution to Eqn. (5) by solving with Orthogonal Matching Pursuit Algorithm (OMP) as given in Eqn. (6)

$$\hat{\mathbf{x}}(k) = \arg\min_{\mathbf{x}(k)} \|\mathbf{y}(k) - \mathbf{\Phi}(k)\mathbf{x}(k)\|_2^2 \quad s.t. \quad \|\mathbf{x}\|_0 < \lambda \quad (6)$$

where λ is the bound on the ℓ_0-norm of the sparse vector $\mathbf{x}$. Now recovered $\hat{\mathbf{x}}(k)$ will be used by the central controller to generate ORPC control input for the control area of power system.

The working of CS based centralized control strategy is explained in Fig. 2, which shows the compression of $\mathbf{x}(k)$ before transmitting it through communication channel. At the
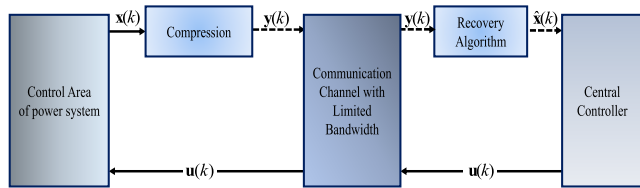
FIGURE 2. CS based centralized control scheme.

end of communication channel it can be recovered using OMP recovery algorithm as proposed in (6).

III. DETAILED WORKING OF COMPRESSIVE SENSING

In this paper, matrices are represented by bold and italic letters, vectors are represented by bold letters whereas scalar quantity is neither bold nor italic. The theory of CS states that a sparse or compressible signal can be recovered with high probability from a few measurements, which is far smaller than the size of the original signal. Power system state signals, having spatial-temporal correlation, thus, can be regarded as compressible. For a control area with n sensors, a data window $X(k)$ which contains $w \geq 1$ consecutive readings of n sensors at the time step k is given as

$$X(k) = \begin{bmatrix} x_1(k-w+1) & \cdots & x_1(k) \\ \vdots & \ddots & \vdots \\ x_n(k-w+1) & \cdots & x_n(k) \end{bmatrix} \quad (7)$$

Denote the ith row of $X(k)$ by $\mathbf{x}_{r,i}(k) = [x_i(k - w + 1), \ldots, x_i(k)]^T$, which contains readings of sensor i at time steps $\{k - w + 1, \ldots, k\}$. Similarly, denote the jth column of $X(k)$ by $\mathbf{x}_{c,j}(k - w + j) = [x_1(k-w+j), \ldots, x_n(k)]^T$, which contains the readings of all sensors i at the time step $k - w + j$.

If there exists a basis $\mathbf{\Psi}_S \in R^{n*n}$ and a basis $\mathbf{\Psi}_T \in R^{w*w}$ for spatial and temporal domains respectively, $X(k)$ can be written in a compressible expression using spatial basis as (8)

$$X(k) = \mathbf{\Psi}_S \theta_S(k) \quad (8)$$
$$\theta_S(k) = [\theta_S(k - w + 1), \ldots., \theta_S(k)]_{n \times w} \quad (9)$$

where $\theta_S(k) \in \mathbf{R}^n$ contains the spatial transform coefficients of n sensors at the time step k and $\theta_S(k)$ is its matrix for the whole data window of w. Similarly, $X(k)$ can also be written in a compressible expression using its temporal basis as

$$X^T(k) = \mathbf{\Psi}_T \theta_T(k) \quad (10)$$
$$\theta_T(k) = [\theta_{T,1}(k)....\theta_{T,n}(k)]_{w \times n} \quad (11)$$

where $\theta_{T,i}(k) \in \mathbf{R}^w$ contains the temporal transform coefficients of sensor i for all w steps.

Kronecker sparsifying bases can succinctly combine the individual sparsifying bases of each signal dimension into a single transformation matrix [36], [39]. Hence, we can merge the transformations in (8) and (10), and represent $X(k)$ as

$$
\begin{aligned}
\mathbf{x}(k) = vec(X(k)) &= vec(\mathbf{\Psi}_S \theta_S(k)) \\
&= vec(\mathbf{\Psi}_S \theta_S(k) \mathbf{\Psi}_T^{-T} \mathbf{\Psi}_T^T) = vec(\mathbf{\Psi}_S \mathbf{Z}(k) \mathbf{\Psi}_T^T) \\
&= (\mathbf{\Psi}_S \otimes \mathbf{\Psi}_T^T) vec(\mathbf{Z}(k)) = \mathbf{\Psi} \mathbf{z}(k) \quad (12)
\end{aligned}
$$

where $\mathbf{\Psi} = (\mathbf{\Psi}_T \otimes \mathbf{\Psi}_S) \in \mathbf{R}^{nw \times nw}$ is the Kronecker sparsifying basis and $\mathbf{z}(k)$ contains the joint transformation domain coefficients. $\mathbf{x}(k) = [\mathbf{x}_{c,1}^T(k-w+1), \ldots, \mathbf{x}_{c,n}^T(k)]^T$ is vector–reshaped data window of $X(k)$, $\mathbf{Z}(k)$ can be interpreted as the matrix representation of spatial domain $\theta_S(k)$ in temporal basis $\mathbf{\Psi}_T$, i.e. $\theta_S^T(k) = \mathbf{\Psi}_T \mathbf{Z}^T(k)$.

It should be noted that any universal data independent basis can be considered as $\mathbf{\Psi}_S$ and $\mathbf{\Psi}_T$. Some of the transformations found suitable for revealing the underlying sparsity of many natural signals include the discrete Fourier transform (DFT) basis, discrete cosine transform (DCT) basis and the discrete wavelet transform (DWT), etc.

$\mathbf{x}(k)$ can be represented by $\mathbf{\Psi}_T \mathbf{z}(k)$ in (4) and (6) for encoding and decoding of the system data respectively. For recovery of the state measurements by (6), initially $\hat{\mathbf{z}}(k)$ will be recovered and then $\hat{\mathbf{x}}(k)$ can be reconstructed using (13)

$$\hat{\mathbf{x}}(k) = \mathbf{\Psi} \hat{\mathbf{z}}(k) \quad (13)$$

Flowchart of the proposed CS based data transmission algorithm is shown in Fig. 3, which shows the steps required to transmit the data using CS.
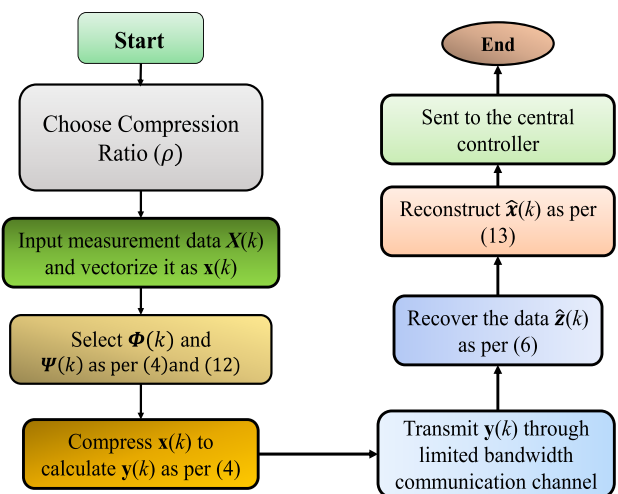

FIGURE 3. Proposed CS based data transmission algorithm.

The performance of CS is mainly evaluated by two criterions:

1. Compression ratio (ρ):

$$\rho = \frac{\text{size of data being transmitted without CS}}{\text{size of data being transmitted with CS}} \quad (14)$$

2. Signal to error ratio (SNR):

$$SNR = -20(\log \|\mathbf{x} - \hat{\mathbf{x}}\|)/\|\mathbf{x}\| \quad (15)$$

where $\mathbf{x}$ is the original signal, $\hat{\mathbf{x}}$ is the recovered signal. The compression ratio (ρ) decides the size of the measurement matrix. It decides the number of rows (m) in the measurement matrix as given in (4). Higher the compression ratio, lower the amount of data to be transmitted on the communication channel.

IV. PROPOSED ORPC ALGORITHM

Optimization of the multi-objective function of (1) can be performed using optimal reactive power control of the generators. However, the inequality constraints of reactive power generation limits should be included to ensure that the reactive power generator limits are not violated. Here, reactive power optimization can be solved using Interior Point Method (IPM) algorithm [40], [41], as given in (16a) [42].

$$\min_{\mathbf{x}} \quad f(\mathbf{x})$$
$$s.t. \quad \mathbf{x} \leq \mathbf{x}_u$$
$$\mathbf{x} \geq \mathbf{x}_l \tag{16}$$

$$P_{Gi} - P_{Li} - V_i \sum_{j=1}^{n} V_j Y_{ij} \cos(\delta_i - \delta_j + \theta_{ij}) = 0 \tag{16a}$$

$$Q_{Gi} - Q_{Li} + V_i \sum_{j=1}^{n} V_j Y_{ij} \sin(\delta_i - \delta_j + \theta_{ij}) = 0 \tag{16b}$$

where $\mathbf{x}_{ui}$ and $\mathbf{x}_{li}$ are the maximum and minimum rated capacities of state variable for bus *i*. $\mathbf{x} = [\mathbf{x}_1, \ldots, \mathbf{x}_n]$, $\mu > 0$ is the vector of barrier parameters which keeps on decreasing until the optimal solution is achieved. (16a & b) are the power flow constraints which need to be satisfied during the control operation and can be written as $c(\mathbf{x})$ in a compact form. These constraints can be included in the formulation using lagrangian approach. Lagrangian of (16a) can be written as (17)

$$L(\mathbf{x}, \lambda, \mathbf{w}_l, \mathbf{w}_u) = f(\mathbf{x}) + c(\mathbf{x})^T \lambda - \mathbf{w}_l^T(\mathbf{x} - \mathbf{x}_l) - \mathbf{w}_u^T(\mathbf{x}_u - \mathbf{x}) \tag{17}$$

(16a) consists of nonlinear equality constraints. It is convenient to utilize a Primal-dual based Interior Point method (PDIPM) to solve nonlinear optimization problems with equality constrains. Hence, the primal-dual equation of (16a) is given as (18a) [43]

$$g(\mathbf{x}) + \mathbf{A}(\mathbf{x})\lambda - \mathbf{w}_l + \mathbf{w}_u = 0 \tag{18}$$
$$c(\mathbf{x}) = 0 \tag{18a}$$
$$(X - X_l)\mathbf{w}_l - \mu\mathbf{e}_l = 0 \tag{18b}$$
$$(X_u - X)\mathbf{w}_u - \mu\mathbf{e}_u = 0 \tag{18c}$$

where g(x) is the dual of $f_1(\mathbf{x})$. λ is the vector of equality constraint dual variables. $\mathbf{w}_l$ and $\mathbf{w}_u$ are the vectors of non-negative dual variables of inequality constraints. X_u and X_l are the matrix of maximum and minimum limits of state variables for a specified window length as given in (7). $\mathbf{e}_l$ and $\mathbf{e}_u$ are two indicator variables to restrict states within feasible regions.

For a fixed u at each iteration and counted by k, the solution of (16a) can be achieved by Newton method where search directions of states can be calculated as (19) [44]

$$\begin{bmatrix} \mathbf{H}(k) & \mathbf{A}(k) \\ \mathbf{A}^T(k) & 0 \end{bmatrix} \begin{bmatrix} \mathbf{d}_\mathbf{x}(k) \\ \mathbf{d}_\lambda(k) \end{bmatrix} = \begin{bmatrix} \nabla f(\mathbf{x}(k)) + \mathbf{A}(k)\lambda(k) \\ c(k) \end{bmatrix} \tag{19}$$

where $\mathbf{d}_\mathbf{x}(k)$ and $\mathbf{d}_\lambda(k)$ are vectors of search direction of $\mathbf{x}$ and λ. Here, $\mathbf{H}(k)$ is a matrix given by (20)

$$\boldsymbol{H}(k) = \boldsymbol{V}(k) + \boldsymbol{W}_l(k)(\boldsymbol{X}(k) - \boldsymbol{X}_l))^{-1} + \boldsymbol{W}_u(k)(\boldsymbol{X}_u - \boldsymbol{X}(k))^{-1} \tag{20}$$

where $\mathbf{V}(k)$ is the Hessian of Langrangian of (17). $\boldsymbol{X}(k)$ is the matrix of state information as given in (7). $\boldsymbol{W}_l$ and $\boldsymbol{W}u$ are the matrices of non-negative dual variables of inequality constraints for a window length of w. In case of using CS to transmit network data to the central controller, rate of compression and recovery is usually very high. Thus, it is reasonable to approximate the gradient and Hessian of function of f_1 numerically as

$$\frac{\partial L}{\partial \mathbf{x}}(\mathbf{k}) = \frac{L(k) - L(k-1)}{\mathbf{x}(k) - \mathbf{x}(k-1)} \tag{21}$$

$$\frac{\partial^2 L}{\partial \mathbf{x}^2}(k) = \frac{\frac{\partial L}{\partial \mathbf{x}}(k) - \frac{\partial L}{\partial \mathbf{x}}(k-1)}{\mathbf{x}(k) - \mathbf{x}(k-1)} \tag{22}$$

Similarly, search direction of the dual variables can be calculated as given in (23a) & (23b)

$$\mathbf{d}_{\mathbf{w}_l}(k) = \mu(k)(X(k) - X_l)^{-1}\mathbf{e}_l - \mathbf{W}_l(k) - \mathbf{w}_l(k)(X(k) - X_l)^{-1}\mathbf{d}_\mathbf{x}(k)) \tag{23a}$$
$$\mathbf{d}_{\mathbf{w}_u}(k) = \mu(k)(X_u - X(k))^{-1}\mathbf{e}_u - \mathbf{w}_u(k) - \mathbf{W}_u(k)(X_u - X(k))^{-1}\mathbf{d}_\mathbf{x}(k)) \tag{23b}$$

Finally, update of next iteration of PDIPM can be obtained by (24(a-d))

$$\mathbf{x}(k+1) = \mathbf{x}(k) + \alpha(k)d_\mathbf{x}(k) \tag{24a}$$
$$\lambda(k+1) = \lambda(k) + \alpha(k)\mathbf{d}_\lambda(k) \tag{24b}$$
$$\mathbf{w}_l(k+1) = \mathbf{w}_l(k) + \alpha(k)\mathbf{d}_{\mathbf{w}_l}(k) \tag{24c}$$
$$\mathbf{w}_u(k+1) = \mathbf{w}_u(k) + \alpha(k)\mathbf{d}_{\mathbf{w}_u}(k) \tag{24d}$$

where $\alpha(k)\epsilon(0, 1]$ is the step size. In classical PDIPM, μ is decreased at each iteration by using a fixed decrement ratio which may slow down the convergence speed of the algorithm. In this paper, authors propose an improved version of PDIPM which decreases the barrier parameter at a super linear rate by using (25)

$$\mu(k+1) = \max\left\{\frac{\varepsilon_{tol}}{\beta}, \min\{\kappa_\mu\mu(k), \mu(k)^{\tau_{\mu(k)}}\}\right\} \tag{25}$$

where ε_{tol} is the given tolerance, $\beta\kappa_\mu\tau_{\mu(k)}\epsilon(5, 15)$, $\epsilon(0, 1)$, and $\epsilon(1, 2)$. To check the convergence of the proposed improved PDIPM, error can be calculated by finding the maximum violation in the primal-dual equations as given in (26)

$$\mathrm{E}_\mu = \max \left\{ \begin{array}{l} \|g(\mathbf{x}) + \mathbf{A}(\mathbf{x})\lambda - \mathbf{w}_l + \mathbf{w}_u\|_\infty/_{S_d}, \|c(\mathbf{x})\|_\infty, \\ \|(\mathbf{x}(k) - \mathbf{x}_l)\mathbf{w}_l - \mu\mathbf{e}_l\|_\infty/s_{c_l}, \\ \|(\mathbf{x}_u - \mathbf{x})\mathbf{w}_u - \mu\mathbf{e}_u\|_\infty/s_{c_u} \end{array} \right\} \tag{26}$$

where s_d, s_{cl} and s_{cu} are the scaling parameters. Detailed working of the proposed improved PDIPM algorithm is provided in Fig. 4.
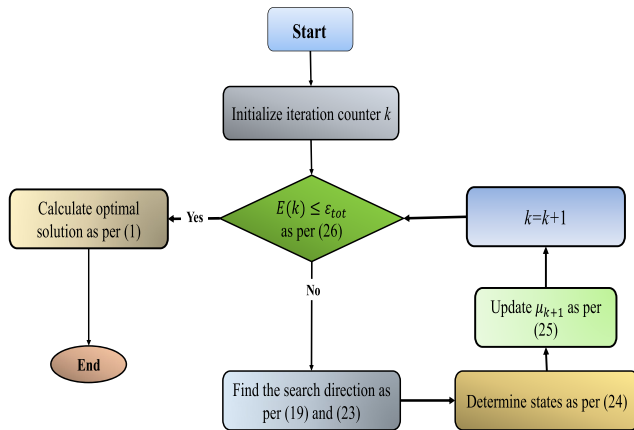
FIGURE 4. Proposed Improved PDIPM algorithm.

It is proved to be an efficient technique for nonlinear constrained optimization and thus, suitable for our optimal reactive power control application. Using improved PDIPM, the central controller needs to collect the real-time data of voltage phasors and power flows which in this case is being achieved by using CS based communication network. After obtaining the real-time data, the central controller generates the optimal control input for each reactive power source in the control area. The optimal control input is the optimal reactive power generation and it is decided based on the minimization of (16a).

Finally, a comprehensive flowchart of the proposed CS based ORPC algorithm is shown in Fig. 5. At the beginning of the algorithm, PDIPM and CS preset parameters are stored in the central controller. Measured data from control area of a power system is compressed as per Fig. 3, before transmitting it through the communication channel. For compression of measured data, two matrices Kronecker sparsifying basis (Ψ) and measurement matrix $\Phi(k)$ are required. Ψ is achieved by taking Kronecker tensor product of Discrete Cosine Transform basis. Measurement matrix $\Phi(k)$ depends on the selected compression ratio for each simulation. If compression ratio rises, number of the rows in the measurement matrix decreases. It is obtained dynamically for each iteration by randomly selecting a sparse matrix with only one non-zero value in each row.

At the end of communication channel, $\hat{\mathbf{z}}(k)$ is recovered using OMP algorithm applied on (27).

$$\mathbf{y}(k) = \Phi(k)\Psi\hat{\mathbf{z}}(k) \qquad (27)$$

It is an under-determined system of equations and is solved using the method of least squares to get an estimate of the solution. However, the information of the sparsity for $\hat{\mathbf{z}}(k)$ does help to derive a more deterministic solution set by incorporating λ with the optimization problem as given in (28) [45].

$$\min_{\hat{\mathbf{z}}(k)} \quad \left\| \Phi(k)\Psi\hat{\mathbf{z}}(k) - \mathbf{y}(k) \right\|_2^2$$
$$s.t. \quad \left\| \hat{\mathbf{z}}(k) \right\|_0 \le \lambda \qquad (28)$$
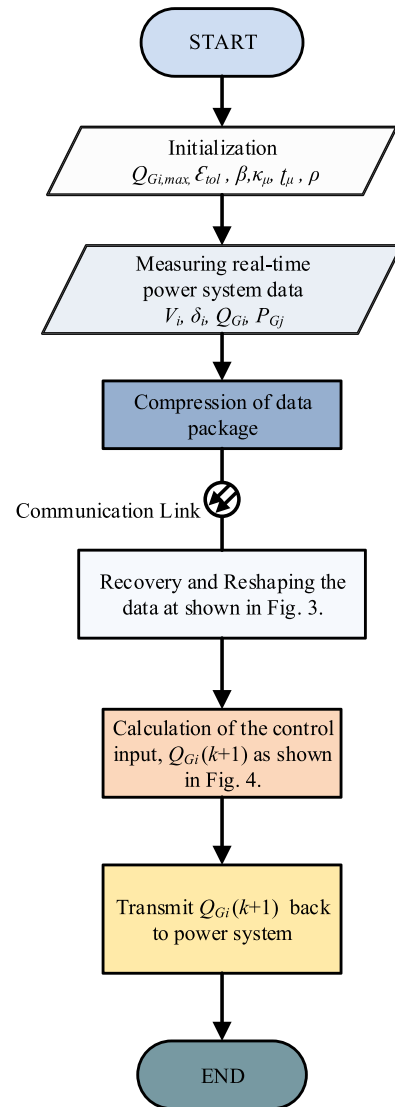

FIGURE 5. 5. Comprehensive flowchart of the proposed CS based ORPC approach.

where λ is the number of non-zeros in the least squares problem and optimal λ is calculated by solving (29)

$$\lambda = \left\| 2\left[\Phi(k)\Psi \right]^T \mathbf{y}(k) \right\|_\infty \qquad (29)$$

Calculation of λ is very important in the recovery algorithm of CS and performance of CS widely depends on the selection of λ. SNR ratio of the recovered signal decreases if we choose value of λ away from optimal value.

After $\hat{\mathbf{z}}(k)$ is achieved using above recovery algorithm, it is reshaped using (13) as explained in chapter III. Then at the central controller, control input $Q_{Gi}(k + 1)$ is generated using improved PDIPM as explained in Fig. 4. Finally, the generated control input is sent back to the control area of power system to improve the objective function (1).

V. SIMULATION STUDIES
In this section, 3 different case studies of 18 bus, 129 bus and 486 bus power system are presented to test effectiveness of

CS for various sizes of control area. Each power system is obtained by combing multiple control areas through tie lines to test the proposed algorithm for multi-area power systems.
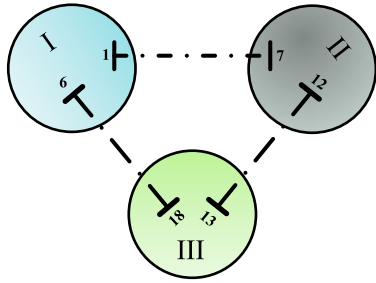

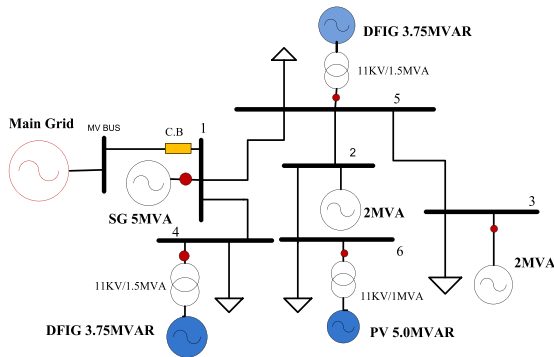**FIGURE 6.** A power system of 18 buses with 6-bus in each control area.

FIGURE 7. 6-bus radial distribution network used as one control area.

A. 18-BUS SYSTEM

The proposed algorithm is applied to a multi-area power system of 18-bus network as shown in Fig. 6. It is built by connecting 3 control areas with 6-bus radial system in each area as shown in Fig. 7. The impedances for all the tie-lines are set to 0.02+j0.07 p.u. In the first control area, bus 1 is a slack bus of the power system and it is connected to the main grid. Three generators with reactive power ranges −3.75 to 3.75MVAR, −3.75 to 3.75 MVAR and −5.0 to 5.0 MVAR are attached at buses 4, 5 and 6, respectively. Reactive power generation from these DGs is utilized to minimize the power loss and voltage deviation of the system, taking the reactive power generation cost into account simultaneously. Reference voltages for 6 buses are assigned as [1.04 1.025 1.025 1.0 1.01 1.015] in an ascending order. Weight coefficients for Power loss, voltage deviation and reactive power cost are set as $W_1 = 0.2$, $W_2 = 100$ and $W_3 = 1.0$, respectively. To analyze the real-time dynamic behavior of CS based ORPC approach, a sequence of load changing events are launched as given in Table 1.

To begin with, the first load change is initiated on bus 5, 11 and 17 by doubling the reactive power load at 12s. The increased load is compensated by the reactive power generation source at bus 5, 11 and 17 as shown in Fig. 8. Similarly, decrease in reactive power load and change in real

TABLE 1. Event sequences of load changes on 18-Bus power system.

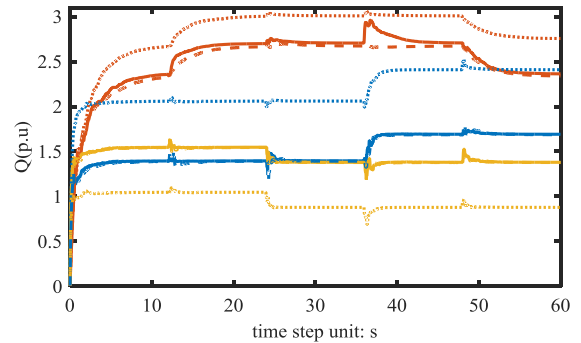| Events	Time stamp	Bus No	Load Type	Load Change
Event1	12s	5,11,17	Reactive Load	2.0×Initial
Event2	24s	6,12,18	Reactive Load	0.5×Event1
Event3	36s	4,10,16	Real Load	1.1×Event2
Event4	48s	5,11,17	Real Load	0.95×Event3

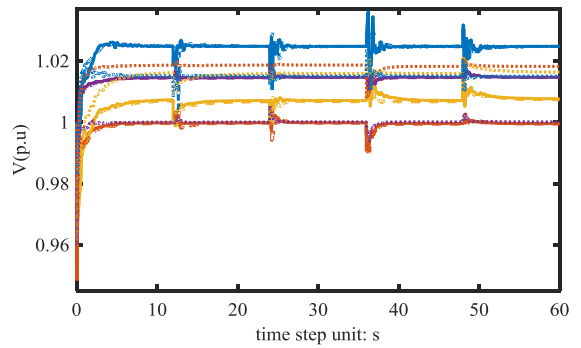**FIGURE 8.** Reactive power generation updates of 9 generators for 18-bus system.

FIGURE 9. Voltage improvement of the non-PV buses for 18-bus system.

power load is counteracted by their respective generators. Fig. 9 shows that none of the above changes in load has introduced significant long-term voltage deviation on any of the bus voltage and all the voltages return to their original optimal values, immediately after the load change. Buses regained their initial optimal values because controllable reactive power sources adjusted their reactive power generation to maintain the optimal bus voltages. Convergence of the proposed algorithm in case of varying loading conditions shows that CS works even when the events of load change occurs in the multi-area power system.

CS has been used to transmit the network data to the central controller. Difference in the voltage updates of two cases: with and without CS is shown in Fig. 10, in which only a small error (of the order of 10^{-3}) is observed in voltage updates during the load variation period. However, after the algorithm reaches the steady-state load condition, error in the voltage vanishes. It is inferred that the proposed CS based approach does not affect the optimal control setting of the reactive power; at the same time, decreasing the data size. Commonly,
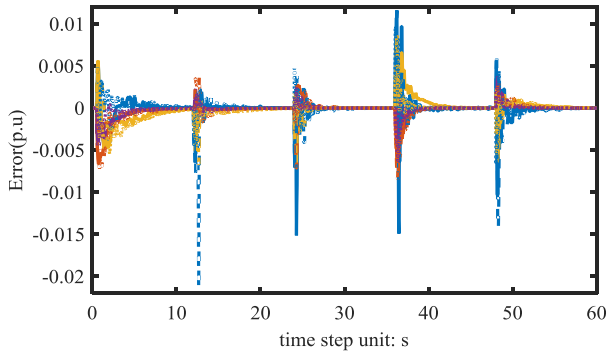
FIGURE 10. Error in the voltage updates with CS.

the power system operates in the steady state condition with only few dynamics in the whole day. It can be concluded that CS is an excellent means of reducing the data size of power system real-time data without affecting the control settings.
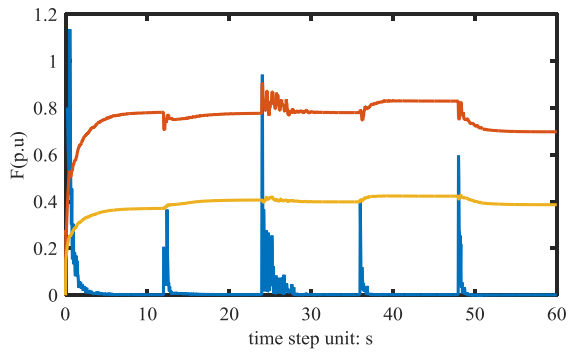

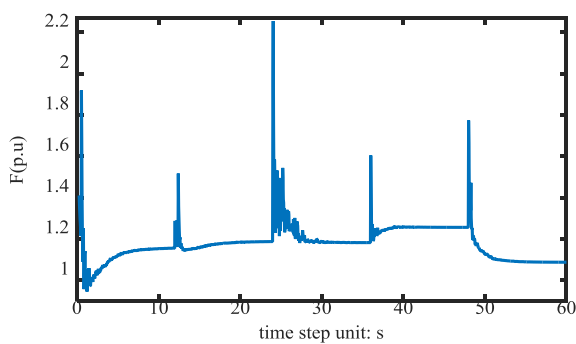**FIGURE 11.** Updates of the individual sub-function.

FIGURE 12. Minimization of the overall objective function.

Figs. 11 & 12 show the updates of each sub-function and the overall objective function, respectively. The reactive power generation increases as reactive power load rises on bus 5, 11 and 17 at 12s. In comparison, the reactive power generation decreases when reactive power load declines at 24s. A rise in real power load increases reactive power cost and power loss of the network. A significant decrease in the reactive power cost and power loss is observed at 48s

when real power load is reduced. According to the power system theory, the less real power demand is, the lower real power loss will be, which in turn, decreases the reactive power demand in the network.

To analyze the effect of compression ratio (ρ) on the recovered signal, OPRC algorithm was initially implemented without CS. After that, CS based ORPC algorithm was simulated with varying compression ratios. Results from both algorithms are compared in Fig. 13 which shows the error in voltage of bus 18 of area 3 by changing the compression ratio. It is clear that higher the compression ratio, more is the error in the voltage. For large compression ratios, proposed algorithm takes more time to converge. Thus, large compression ratio makes the algorithm slow down but converges to same optimal value. It is noteworthy that in small power system, the achievable compression ratio is small.
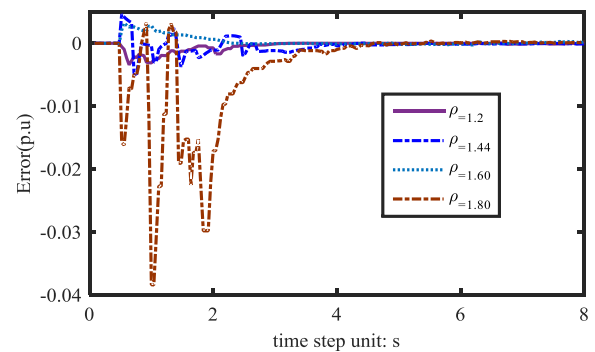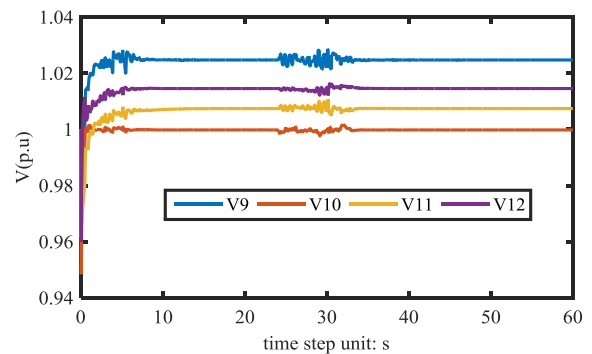

FIGURE 13. Error in V_{18} with the use of CS.

FIGURE 14. 14 Voltage updates of area 2 with white noise of SNR=50 on V10.

B. EFFECT OF RANDOM DISTURBANCE
Effect of random disturbance is studied by introducing random white noise in the voltage of bus 10 in area 2 from 25s to 33s as shown in Fig.14 where white noise with SNR=50 is added. It is observed that adding random disturbance in the voltage of one bus introduces disturbance in the neighboring buses as well. It validates our assumption that power system states have spatial correlation in them and thus are compressible. To analyze the behavior of proposed ORPC algorithm in
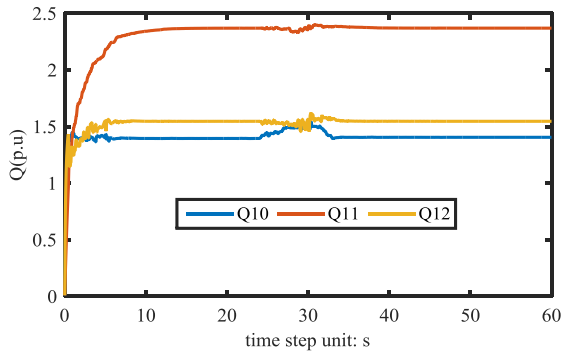
FIGURE 15. Reactive power updates of area 2 with white noise of SNR=50 in V_{10}.

presence of random disturbances, reactive power generation updates are shown in Fig. 15. It shows that all generators in area 2, particularly generator on bus 10 act by changing their generation to deal with any abrupt random disturbances.
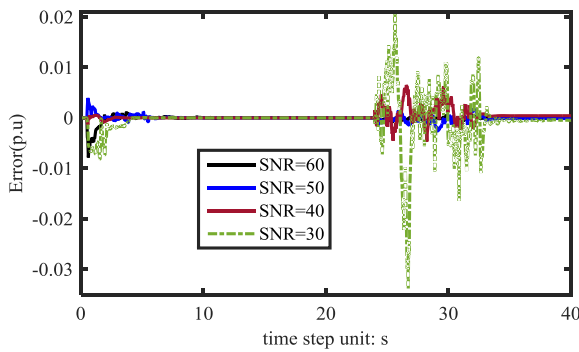

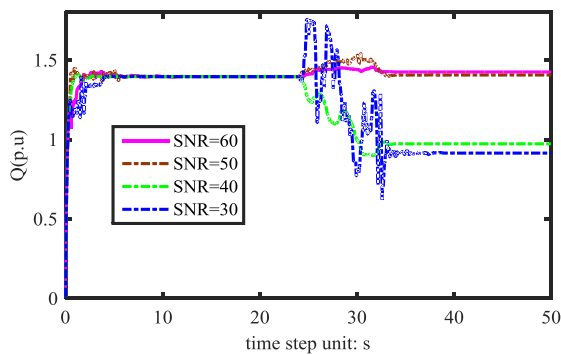**FIGURE 16.** Error in V10 for different SNR ratios.

FIGURE 17. Reactive power generation updates of bus 10 for different SNR ratios.

To study the effect of random disturbances of higher magnitudes on the recovered data, SNR ratio was decreased from 60 to 30, as shown in Fig. 16. Fig. 16 exhibits that when the random disturbance increases in the system states, error in the recovered data rises. Similar response is observed in the reactive power generation updates as shown in Fig. 17, which shows reactive power generation output of bus 10 for different SNR.
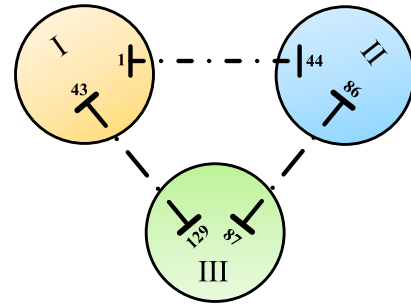

FIGURE 18. A power system of 129 buses with 43-bus in each control area.

C. 129-BUS POWER SYSTEM

CS is used to deal with the signals from the 129-bus power system as shown in Fig. 18 formed by connecting three 43-bus control areas, with the line data and bus data as given in [46]. In each area, 14 controllable reactive power generators attached on [3, 5, 7, 12, 14, 16, 18, 20, 24, 26, 27, 38, 41, 42] buses are used for ORPC. Voltages of non-PV buses and line currents are taken as the data for transmission through communication channel using CS. Real-time load changes are introduced on several buses, as shown in Table 2.

TABLE 2. Event sequences of load changes on 129-bus power system.

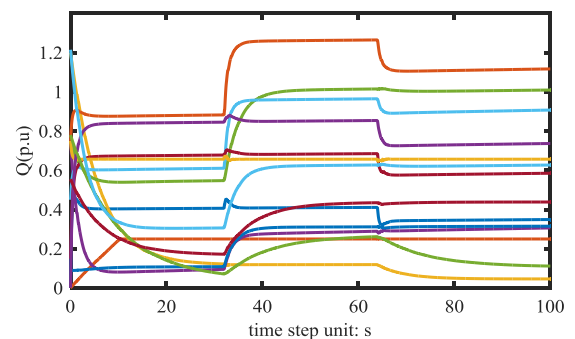| Events	Time	Bus No.	Load Type	Load Change
Event1	33s	[12,14,16,20,24,38,41,42,55,57,59,63,67,81,83,85,98,100,102,106,110,124,126,128]	React. Load	1.6*Initial
Event2	66s	[12,14,16,20,24,38,42,55,57,59,63,67,81,85,98,100,102,106,110,124,126,128]	Real Load	0.5*Event1

FIGURE 19. Reactive power updates of 14 generators.

Reactive power generation updates, as shown in Fig. 19, converge to their optimal values before a dynamic load change occurs at 33s, when reactive power generation increases, as exhibited in Figs. 19 & 22. This rise in reactive power load causes the voltage dip for a very short interval and it immediately recovers its optimal voltage profile by applying the proposed approach, as shown in Fig. 20. Similar behavior is observed when real power load demand is reduced
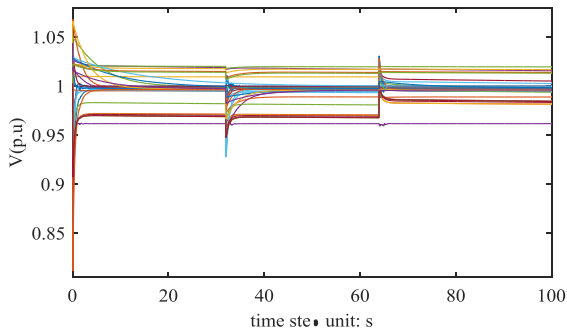
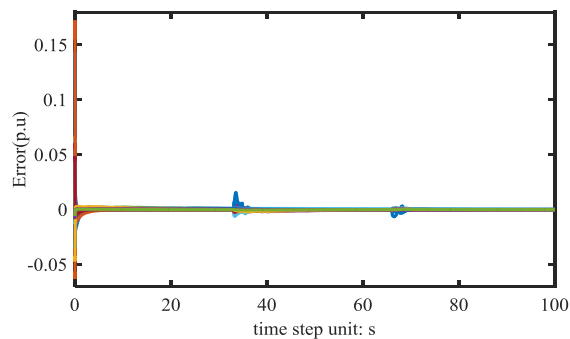**FIGURE 20.** Voltage improvement of the 33 non-PV buses in area 2.

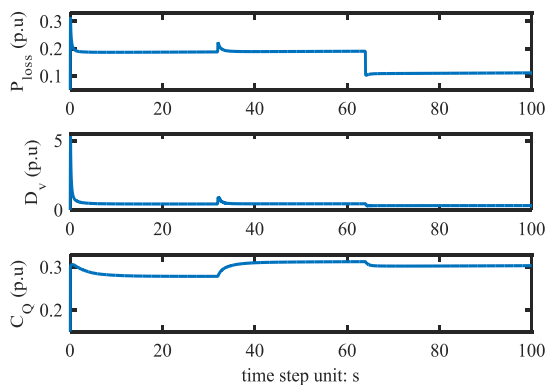**FIGURE 21.** Error in the voltage updates of the 33 non-PV buses.

FIGURE 22. Updates of the individual sub-functions for 129-bus power system.

FIGURE 23. Minimization of the overall objective function.

FIGURE 24. Large power system of 648 buses with 162-bus in each control area.

D. 648- BUS POWER SYSTEM

In order to test the proposed algorithm's performance with a large scale control area, a test case on 648-bus power system, built by connecting 4 areas with 162-buses each as shown in Fig 24, is conducted here. Parameters of 162-bus system can be found in [47]. The resistance and reactance for all the tie-lines are set to 0.028 p.u and 0.096 p.u., respectively. The overall system has 1144 branches and 200 reactive power generation controllers, with 50 reactive power controllable sources in each control area. 153 buses are non-PV buses, and their state information data needs to be transmitted to the central controller for controlling the 50 reactive power sources. Reactive power loads on buses [15, 21, 22, 23, 27, 36, 67, 68, 84, 89, 94, 98, 137, 142, 148] are increased to 1.6 times of their initial values at 100s to test the system's dynamic behavior under the proposed approach.

Update of reactive power generation using CS for data transmission is shown in Fig. 25, which shows increase in its generation at 100 s when the reactive power load is increased. Fig. 26 shows the convergence of the error to zero, immediately after the load change. Subjected to an abrupt increase in the reactive load, bus voltages deviate from their reference voltages and thus voltage deviation is increased. Similar increase is observed in power loss when load increases at 100s, as shown in Fig. 27.

by 0.6 times of the initial load. Reactive power generation cost decreases as can be observed in Fig. 22. Notice that, the fall in real power demand at 66s reduces the current flow through the network, which in turn, reduces power loss, reactive power generation requirement and hence reduces the overall objective function, as shown in Fig. 23.

The result in Fig. 21 exhibits the effectiveness of the proposed CS based approach as the difference for the state variables for the two cases: with and without using CS, converges to zero within a few seconds of any dynamic change. Results in Figs. 19-22 of reactive power generation, voltage magnitudes and objective function, all are obtained using CS based control scheme, which validates the effectiveness of using compressive sensing for ORPC.
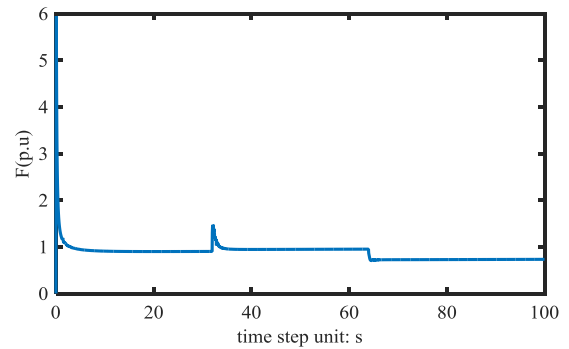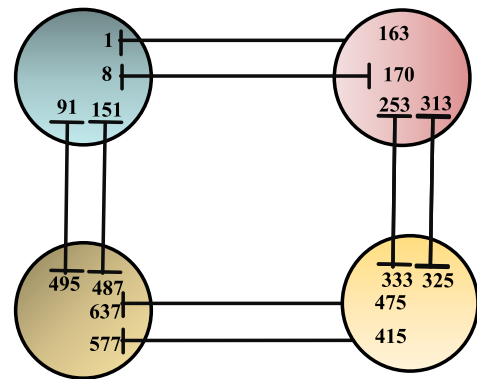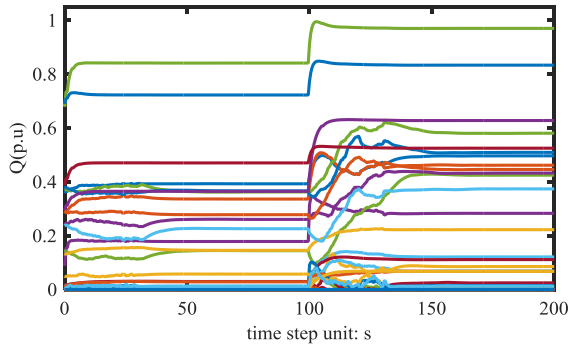
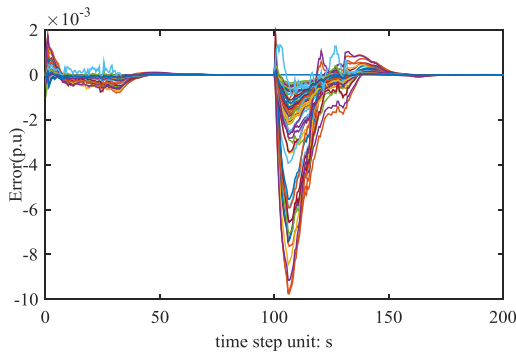**FIGURE 25.** Reactive power updates of 50 reactive power controllers.

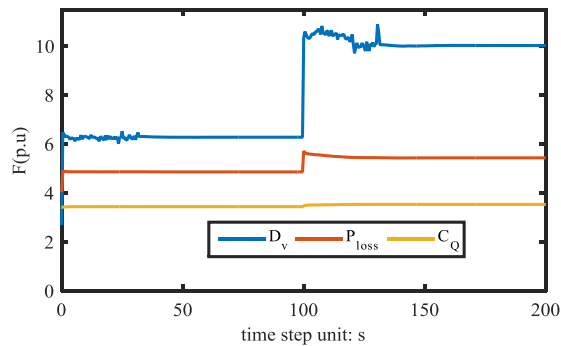**FIGURE 26.** Error in the voltage updates.

FIGURE 27. Updates of three sub-objective functions.

E. ANALYSIS OF CHOOSING OPTIMAL λ AND ITS EFFECT ON THE RECOVERED DATA

λ is the number of non-zeros used in the least squares problem of data recovery and it has an optimal value for each power system. If λ used in OMP problem changes from the optimal λ, the recovered signal may be of poor quality. To visualize its effect on the signal quality, various values of λ are used and corresponding SNR value of the recovered signal is measured as shown in Fig. 28. It shows that each power system has an optimal value of λ for which SNR value is the highest. For rest of the λs, quality of the recovered signal decreases. It also exhibits that λ changes with the size of power system. For large power systems, amount of data transfer is large and thus optimal λ will be large for high quality signal recovery.
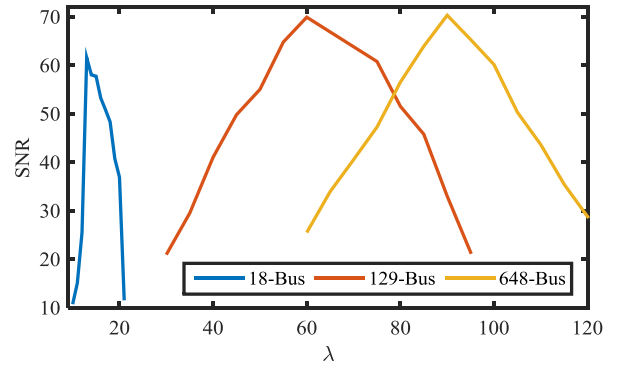

FIGURE 28. Effect of λ on the quality of the recovered signal.

F. EFFECT OF THE COMPRESSION RATIO ON THE RECOVERED DATA

Each of the three case studies is tested for various compression ratios and it is observed that by increasing the compression ratio, the quality of recovered signal is affected.
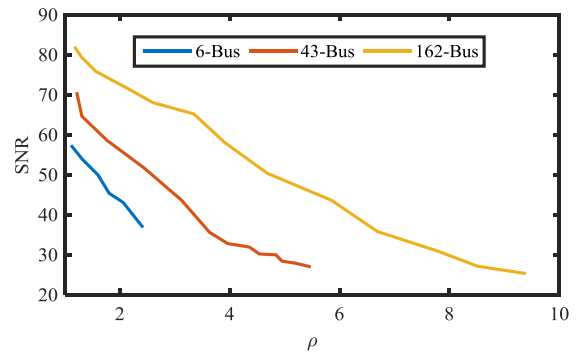

FIGURE 29. Curves showing the relation between ρ and SNR for the three cases.

Fig. 29 shows the curves between SNR and the compression ratio for the three case studies, which exhibits that SNR drops as the compression ratio increases. It is also shown that as the network size increases, the value of achievable compression ratio grows i.e. the values of achievable compression ratio for 6-bus, 43-bus and 162-bus control areas are 2.4, 5.445 and 9.3636, respectively. Thus, the proposed CS based approach is promising for the large system applications where data size can be reduced to 1/9 of the original size.

VI. CONCLUSIONS

Issue of limited-bandwidth communication network in ORPC has been addressed by using CS for data transmission from dispersed control areas to the central controller. OMP based algorithm, which can significantly accelerate the recovery speed, is utilized to recover the data at the receiving end of communication channel. It is shown that data size can be reduced 1/9 times with the help of CS without deteriorating the performance of the proposed approach using CS.

Three case studies are presented, ranging from small to large power systems, to validate the effectiveness of the proposed CS based approach for ORPC problem. Various load changes are introduced to different buses in the network to test the performance of the proposed approach on the real time power system. It is observed that difference in the state variables (with and without using CS) approaches to zero, immediately after the occurrence of load changes. The value of achievable compression ratio is higher for the large control areas than that of the small control areas, which indicates the promising applications of the proposed approach in the large systems. Error in the recovered data depends on the compression ratio of the measurement matrix. It also varies with number of non-zero values taken in the recovery algorithm. Recovery algorithm has an optimal number of non-zeros for each power system. Any deviation from this value will cause rise in the error of the recovered data.

REFERENCES

[1] W. Zheng, W. Wu, B. Zhang, H. Sun, and Y. Liu, "A fully distributed reactive power optimization and control method for active distribution networks," *IEEE Trans. Smart Grid*, vol. 7, no. 2, pp. 1021–1033, Mar. 2016.

[2] Verizon. (2015). *State of the Market: The Internet of Things 2015*. Accessed: Dec. 22, 2016. [Online]. Available: http://www.verizonenterprise.com/state-of-the-market-internet-of-things/

[3] H. Gharavi and B. Hu, "Scalable synchrophasors communication network design and implementation for real-time distributed generation grid," *IEEE Trans. Smart Grid*, vol. 6, no. 5, pp. 2539–2550, Sep. 2015.

[4] S. Das and T. S. Sidhu, "Application of compressive sampling in synchrophasor data communication in WAMS," *IEEE Trans Ind. Informat.*, vol. 10, no. 1, pp. 450–460, Feb. 2014.

[5] M. Qiu, W. Gao, M. Chen, J.-W. Niu, and L. Zhang, "Energy efficient security algorithm for power grid wide area monitoring system," *IEEE Trans. Smart Grid*, vol. 2, no. 4, pp. 715–723, Dec. 2011.

[6] S. Chen, W. Hu, C. Su, X. Zhang, and Z. Chen, "Optimal reactive power and voltage control in distribution networks with distributed generators by fuzzy adaptive hybrid particle swarm optimisation method," *IET Generat., Transmiss. Distrib.*, vol. 9, no. 11, pp. 1096–1103, Aug. 2015.

[7] W. Zhang, W. Liu, X. Wang, L. Liu, and F. Ferrese, "Distributed multiple agent system based online optimal reactive power control for smart grids," *IEEE Trans. Smart Grid*, vol. 5, no. 5, pp. 2421–2431, Sep. 2014.

[8] A. Colet-Subirachs, A. Ruiz-Alvarez, O. Gomis-Bellmunt, F. Alvarez-Cuevas-Figuerola, and A. Sudria-Andreu, "Centralized and distributed active and reactive power control of a utility connected microgrid using IEC61850," *IEEE Syst. J.*, vol. 6, no. 1, pp. 58–67, Mar. 2012.

[9] K. Turitsyn, P. Šulc, S. Backhaus and M. Chertkov, "Distributed control of reactive power flow in a radial distribution circuit with high photovoltaic penetration," in *Proc. IEEE PES General Meeting*, Minneapolis, MN, USA, 2010, pp. 1–6.

[10] M. E. Elkhatib, R. E. Shatshat, and M. M. A. Salama, "Decentralized reactive power control for advanced distribution automation systems," *IEEE Trans. Smart Grid*, vol. 3, no. 3, pp. 1482–1490, Sep. 2012.

[11] H. K. Nguyen, H. Mohsenian-Rad, A. Khodaei, and Z. Han, "Decentralized reactive power compensation using nash bargaining solution," *IEEE Trans. Smart Grid*, vol. 8, no. 4, pp. 1679–1688, Jul. 2017.

[12] Y. Xu, W. Zhang, and W. Liu, "Distributed dynamic programming-based approach for economic dispatch in smart grids," *IEEE Trans Ind. Informat.*, vol. 1, no. 1, pp. 166–175, Feb. 2015.

[13] S. Bolognani, R. Carli, G. Cavraro, and S. Zampieri, "Distributed reactive power feedback control for voltage regulation and loss minimization," *IEEE Trans. Autom. Control*, vol. 60, no. 4, pp. 966–981, Apr. 2015.

[14] A. Maknouninejad and Z. Qu, "Realizing unified microgrid voltage profile and loss minimization: A cooperative distributed optimization and control approach," *IEEE Trans. Smart Grid*, vol. 5, no. 4, pp. 1621–1630, Jul. 2014.

[15] M. S. Lacher, J. Nonnenmacher, and E. W. Biersack, "Performance comparison of centralized versus distributed error recovery for reliable multicast," *IEEE/ACM Trans. Netw.*, vol. 8, no. 2, pp. 224–238, Apr. 2000.

[16] Q. Wan, W. Zhang, Y. Xu, and I. Khan, "Distributed control for energy management in a microgrid," in *Proc. IEEE/PES Transm. Dist. Conf. Expo. (T&D)*, Dallas, TX, USA, 2016, pp. 1–5.

[17] N. Jumpasri, K. Pinsuntia, K. Woranetsuttikul, T. Nilsakorn, and W. Khan-Ngern, "Comparison of distributed and centralized control for partial shading in PV parallel based on particle swarm optimization algorithm," in *Proc. Int. Elect. Eng. Congr. (IEECON)*, Chonburi, Thailand, Mar. 2014, pp. 1–4.

[18] O. A. Mousavi and R. Cherkaoui, "Maximum voltage stability margin problem with complementarity constraints for multi-area power systems," *IEEE Trans. Power Syst.*, vol. 29, no. 6, pp. 2993–3002, Nov. 2014.

[19] O. A. Mousavi and R. Cherkaoui. (2011). *Literature Survey on Fundamental Issues of Voltage and Reactive Power Control*. [Online]. Available: http://mars.ethz.ch/en/researh-and-publications/publications.html

[20] Y. Phulpin, "Coordination of reactive power scheduling in a multi-area power system operated by independent utilities," Electr. Power, Georgia Inst. Technol., Atlanta, GA, USA, Tech. Rep. tel-00424534, 2009.

[21] O. A. Mousavi and R. Cherkaoui, "On the inter-area optimal voltage and reactive power control," *Int. J. Elect. Power Energy Syst.*, vol. 52, pp. 1–13, Nov. 2013.

[22] M. Alizadeh and R. Cherkaoui, "On voltage and frequency control in multi-area power systems security," Ph.D. dissertation, École Polytechn. Fédérale De Lausanne, Lausanne, Switzerland, 2014.

[23] A. Zhang, H. Li, F. Liu, and H. Yang, "A coordinated voltage/reactive power control method for multi-TSO power systems," *Int. J. Elect. Power Energy Syst.* vol. 43, no. 1, pp. 20–28 2012.

[24] Y. Phulpin, M. Begovic, and D. Ernst, "Coordination of voltage control in a power system operated by multiple transmission utilities," in *Proc. IREP Symp.* Aug. 2010, pp. 1–8.

[25] Z. W. Liu and M. B. Liu, "Distributed reactive power optimization computing in multi-area power systems using ward equivalent," in *Proc. Int. Conf. Elect. Control Eng.*, Wuhan, China, 2010, pp. 3659–3663.

[26] Y. Phulpin, M. Begovic, M. Petit, and D. Ernst, "A fair method for centralized optimization of multi-TSO power systems," *Int. J. Elect. Power Energy Syst.* vol. 31, no. 1, pp. 482–488, 2009.

[27] Y. Phulpin, M. Begovic, M. Petit, and D. Ernst, "On the fairness of centralised decision-making strategies in multi-TSO power systems," in *Proc. Power Syst. Comput. Conf.*, 2008, p. 7.

[28] Y. Phulpin, M. Begovic, and M. Petit, "External network modeling for MVAr scheduling in multi area power systems," in *Proc. Power Tech.*, Jul. 2007, pp. 1039–1043.

[29] Y. Phulpin, M. Begovic, M. Petit, J.-B. Heyberger, and D. Ernst, "Evaluation of network equivalents for voltage optimization in multi-area power systems," *IEEE Trans. Power Syst.* vol. 24, no. 2, pp. 729–743, May 2009.

[30] E. J. Candès and M. B. Wakin, "An introduction to compressive sampling," *IEEE Signal Process. Mag.*, vol. 25, no. 2, pp. 21–30, Mar. 2008.

[31] J. Haupt, W. U. Bajwa, M. Rabbat, and R. Nowak, "Compressed sensing for networked data," *IEEE Signal Process. Mag.*, vol. 25, no. 2, pp. 92–101, Mar. 2008.

[32] Z. Zou, Y. Bao, H. Li, B. F. Spencer, and J. Ou, "Embedding compressive sensing-based data loss recovery algorithm into wireless smart sensors for structural health monitoring," *IEEE Sensors J.*, vol. 15, no. 2, pp. 797–808, Feb. 2015.

[33] Y. Yu, F. Han, Y. Bao, and J. Ou, "A study on data loss compensation of WiFi-based wireless sensor networks for structural health monitoring," *IEEE Sensors J.*, vol. 16, no. 10, pp. 3811–3818, May 2016.

[34] A. Ozdemir, "Loss-constrained economic power dispatch," *IEE Proc.-Generat., Transmiss. Distrib.*, vol. 143, no. 5, pp. 387–392, Sep. 1996.

[35] H. Nezamabadi and M. S. Nazar, "Arbitrage strategy of virtual power plants in energy, spinning reserve and reactive power markets," *IET Generat., Transmiss. Distrib.*, vol. 10, no. 3, pp. 750–763, Mar. 2016.

[36] D. Jiang, L. Nie, Z. Lv, and H. Song, "Spatio-temporal kronecker compressive sensing for traffic matrix recovery," *IEEE Access*, vol. 4, pp. 3046–3053, 2016.

[37] D. Needell and J. A. Tropp, "CoSaMP: Iterative signal recovery from incomplete and inaccurate samples," *Appl. Comput. Harmon. Anal.*, vol. 26, no. 3, pp. 301–321, 2009.

[38] J. A. Tropp and A. C. Gilbert, "Signal recovery from random measurements via orthogonal matching pursuit," *IEEE Trans. Inf. Theory*, vol. 53, no. 12, pp. 4655–4666, Dec. 2007.

[39] M. Leinonen, M. Codreanu, and M. Juntti, "Sequential compressed sensing with progressive signal reconstruction in wireless sensor networks," *IEEE Trans. Wireless Commun.*, vol. 14, no. 3, pp. 1622–1635, Mar. 2015.

[40] J. Zhu, "Reactive power optimization," in *Optimization of Power System Operation*, vol. 1. New York, NY, USA: Wiley, 2009, pp. 409–454.

[41] F. Meng, B. Chowdhury, and M. Chamana, "Three-phase optimal power flow for market-based control and optimization of distributed generations," *IEEE Trans. Smart Grid*, to be published. doi: 10.1109/TSG.2016.2638963.

[42] F. Capitanescu, M. Glavic, D. Ernst, and L. Wehenkel, "Interior-point based algorithms for the solution of optimal power flow problems," *Electr. Power Syst. Res.*, vol. 77, nos. 5–6, pp. 508–517, Apr. 2007.

[43] Z. Yu and D. Pu, "A new nonmonotone line search technique for unconstrained optimization," *J. Comput. Appl. Math.*, vol. 219, no. 1, pp. 134–144, 2008.

[44] L. Wang, X. Liu, and Z. Zhang, "An efficient interior-point algorithm with new non-monotone line search filter method for nonlinear constrained programming," *Eng. Opt.*, vol. 49, p. 2, pp. 290–310, 2017.

[45] Y. C. Pati, R. Rezaiifar, and P. S. Krishnaprasad, "Orthogonal matching pursuit: Recursive function approximation with applications to wavelet decomposition," in *Proc. IEEE Conf. Rec. 27th Asilomar Conf. Signals, Syst. Comput*, Nov. 1993, pp. 40–44.

[46] C. Ahn and H. Peng, "Decentralized voltage control to minimize distribution power loss of microgrids," *IEEE Trans. Smart Grid*, vol. 4, no. 3, pp. 1297–1304, Sep. 2013.

[47] (1993). *Power System Test Case Archive*. [Online] Available: http://www.ee.washington.edu/research/pstca/

Irfan Khan (S' 16) received the B.Sc. degree in electrical engineering from the University of Engineering and Technology, Lahore, Pakistan, in 2009, and the M.Sc. degree in electrical power engineering from the University of Greenwich, London, U.K., in 2011.

He is currently pursuing the Ph.D. degree in electrical and computer engineering with Carnegie Mellon University, Pittsburgh, PA, USA. His research interests include control and optimization of smart energy networks.

YINLIANG XU (M'13) received the B.S. and M.S. degrees in control science and engineering from the Harbin Institute of Technology, China, in 2007 and 2009, respectively, and the Ph.D. degree in electrical and computer engineering from New Mexico State University, Las Cruces, NM, USA, in 2013.

From 2013 to 2014, he was a Visiting Scholar with the Department of Electrical and Computer Engineering, Carnegie Mellon University, Pittsburgh, PA, USA. He was with the School of Electronics and Information Technology, Sun Yat-sen University, from 2013 to 2017. He is currently an Assistant Professor with the Laboratory of Smart Grid and Renewable Energy, Tsinghua-Berkeley Shenzhen Institute, Shenzhen, China. He is also an Adjunct Faculty with the Department of Electrical and Computer Engineering, Carnegie Mellon University. His research interests include distributed control and optimization of power systems, renewable energy integration, and microgrid modeling and control.

Soummya Kar (M'10) received the B.Tech. degree in electronics and electrical communication engineering from IIT Kharagpur, Kharagpur, India, in 2005, and the Ph.D. degree in electrical and computer engineering from Carnegie Mellon University, Pittsburgh, PA, USA, in 2010. From 2010 to 2011, he was with the Electrical Engineering Department, Princeton University, Princeton, NJ, USA, as a Post-Doctoral Research Associate. He is currently an Associate Professor of electrical and computer engineering with Carnegie Mellon University. His research interests include decision-making in large-scale networked systems, stochastic systems, multi-agent systems and data science, with applications to cyber-physical systems and smart energy systems. He has authored extensively in these topics with over 140 articles in journals and conference proceedings and holds multiple patents. He received the 2016 O. Hugo Schuck Best Paper Award from the American Automatic Control Council, the 2016 Dean's Early Career Fellowship from CIT, Carnegie Mellon, and the 2011 A. G. Milnes Award for Best Ph.D. Thesis in electrical and computer engineering, Carnegie Mellon University.

HONGBIN SUN (SM'12) received the double B.S. degrees from Tsinghua University in 1992, the Ph.D. degree from the Department of E.E., Tsinghua University, in 1996.

From 2007 to 2008, he was a Visiting Professor with the School of EECS, Washington State University, Pullman. He is currently the Changjiang Scholar Chair Professor with the Department of E.E. and the Director of Energy Management and Control Research Center, Tsinghua University. He has authored over 400 peer-reviewed papers, within which over 60 are the IEEE and the IET journal papers, and four books. He has been authorized five U.S. Patents of Invention and over 100 Chinese Patents of Invention. His technical areas include electric power system operation and control with specific interests on the energy management system, system-wide automatic voltage control, and energy system integration. He is currently an IET Fellow. He currently serves as the Editor of the IEEE TSG, an Associate Editor of the IET RPG, and a member of the editorial board of four international journals and several Chinese journals.

• • •